Examining the Amine Functionalization in Dicarboxylates: Photoelectron Spectroscopy and Theoretical Studies of Aspartate and Glutamate

ARTICLE *in* THE JOURNAL OF PHYSICAL CHEMISTRY A · JUNE 2014

Impact Factor: 2.69 · DOI: 10.1021/jp505439b · Source: PubMed

THE JOURNAL OF PHYSICAL CHEMISTRY A

Article

pubs.acs.org/JPCA

Examining the Amine Functionalization in Dicarboxylates: Photoelectron Spectroscopy and Theoretical Studies of Aspartate and Glutamate

Shihu H. M. Deng,[†] Gao-Lei Hou,[†,#] Xiang-Yu Kong,[†,#] Marat Valiev,*[,‡] and Xue-Bin Wang*[,†]

[†]Physical Sciences Division, Pacific Northwest National Laboratory, 902 Battelle Boulevard, P.O. Box 999, MS K8-88, Richland, Washington 99352, United States

[‡]Environmental Molecular Sciences Laboratory, Pacific Northwest National Laboratory, P.O. Box 999, Richland, Washington 99352, United States

Supporting Information

ABSTRACT: Aspartate (Asp^{2-}) and glutamate (Glu^{2-}), two doubly charged conjugate bases of the corresponding amino acids, were investigated using low-temperature negative ion photoelectron spectroscopy (NIPES) and ab initio calculations. The effect of amine functionalization was studied by a direct comparison to the parent dicarboxylate species ($^{-}CO_2-(CH_2)_n-CO_2^{-}$, DC_n^{2-}), succinate (DC_2^{2-}) and propionate (DC_3^{2-}). Experimentally, the addition of the amine group for the n = 2 case (DC_2^{2-}, Asp^{2-}) significantly improves the stability of the resultant Asp^{2-} dianionic species, albeit that NIPES shows only a small increase in adiabatic electron detachment energy (ADE) (+0.05 eV). In contrast, for n = 3 (DC_3^{2-}, Glu^{2-}), a much larger ADE increase is observed (+0.15 eV). Similar results are obtained through ab initio calculations. The latter indicates that increased stability of Asp^{2-} can be attributed to the lowering of the energy of the singlet dianion state due to hydrogen bonding effects. The effect of the amino group on the doublet monoanion state is more complicated and results in the weakening of the binding of the adjacent carboxylate group due to electronic structure resonance effects. This conclusion is confirmed by the analysis of NIPES results that show enhanced production of near-zero kinetic energy electrons observed experimentally for amine-functionalized species.

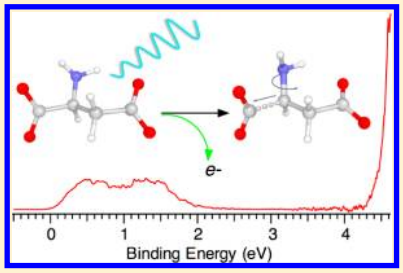

INTRODUCTION

Amino acids consist of a main chain amine group (N-terminus), a main chain carboxylic acid group (C-terminus), and a side chain. The side chain determines the type of the amino acid and its unique properties. Aspartic and glutamic acids, which have a carboxylic group on the side chain, are the two most acidic amino acids and play an important role in biological processes.[1−5] They often directly participate in the enzymatic reactions at the active sites,[1] as well as neurotransmitter[2,3] and ion channel[4,5] functions. The importance of the two species is not limited to biology. For example, monosodium glutamate salt is well-known flavor-enhancing chemical, which has been in use for over 100 years.

Aspartate (Asp^{2-}) and glutamate (Glu^{2-}) can be thought of as amine-functionalized derivatives of succinate (DC_2^{2-}) and propionate (DC_3^{2-}), members of a general family of unbranched dicarboxylate dianons ($^{-}CO_2-(CH_2)_n-CO_2^{-}$, DC_n^{2-}). This class of molecules was among the first multiply charged anions (MCAs) observed in mass spectrometry.[6] Observation of these exotic gaseous species has stimulated and opened up the field in searching and charactering MCAs.[7−12] Using different sizes of $-(CH_2)_n-$ chains allows control of the distance between the two carboxylate charged groups and the overall flexibility of the molecule, providing an ideal MCA system to systematically study effects of intramolecular Coulomb repulsion on electronic structure properties.[13,14] As such, dicarboxylate dianons have been investigated extensively in the past decade employing negative ion photoelectron spectroscopy (NIPES)[13−18] coupled with an electrospray ionization (ESI) source, collision-induced dissociations,[19] and theoretical calculations.[15,19,20] DC_2^{2-} and DC_3^{2-} are the smallest dicarboxylates observed in the experiments, with the former being barely (un)stable against electron detachment, rendering it very difficult to be observed.[14,16]

In contrast to extensively characterized DC_2^{2-} and DC_3^{2-}, no similar study has been reported for Asp^{2-} and Glu^{2-}. The wealth of information and experience accumulated in the investigation of dicarboxylate dianons provides a good foundation for a comparison study on Asp^{2-}/DC_2^{2-} and Glu^{2-}/DC_3^{2-}. Combining experimental NIPES measurements with ab initio calculations, our investigation aims to understand how the addition of the amine group affects the structures and stability of parent dicarboxylate species, gain insight into the changes that accompany the electron detachment process in Asp^{2-} and Glu^{2-}, and characterize resulting monoanion radical $Asp^{\bullet-}$ and $Glu^{\bullet-}$ species. Such information may prove useful to

Received: June 2, 2014
Revised: June 26, 2014
Published: June 30, 2014

   dx.doi.org/10.1021/jp505439b | J. Phys. Chem. A 2014, 118, 5256−5262

better understand their biological roles in various physiological processes.

NEGATIVE ION PHOTOELECTRON SPECTROSCOPY

In this work, a NIPES coupled with an ESI source and a cryogenic ion trap was used to obtain NIPE spectra at 20 K.[21] The dianions of Asp^{2-}, Glu^{2-}, DC_2^{2-}, and DC_3^{2-} were produced using ESI from a 0.1 mM solution of the corresponding acids and NaOH (acid/base molar ratio 1/2) in water/acetonitrile (1/3) solvent. The anions generated were trapped and cooled for 20−100 ms by collision with cold buffer gas molecules (20% H_2 seeded in He) in the ion trap before being transferred into the extraction zone of a time-of-flight (TOF) mass spectrometer. These anions were then mass-selected and decelerated before being photodetached with a laser beam at 355 (3.496 eV) and 266 nm (4.661 eV) from a Nd:YAG laser and 193 nm (6.424 eV) from an ArF excimer laser. The laser was operated at a 20 Hz repetition rate with the ion beam off at alternating laser shots to enable shot-to-shot background subtraction to be carried out. Photoelectrons were collected at ∼100% efficiency (the detachment zone needs to be maintained in ultrahigh vacuum conditions to ensure high collection efficiency for a slow electron as well) with a magnetic bottle and analyzed in a 5.2 m long electron flight tube. The TOF photoelectron spectra were collected and converted to kinetic energy spectra, calibrated using known spectra of I^- and $OsCl_6^{2-}$. The electron binding energy (EBE) spectra were obtained by subtracting the kinetic energy spectra from the detachment photon energies and had a resolution (ΔE/kinetic energy) of ∼2% or 20 meV at 1 eV as measured for I^- at 355 nm.

THEORETICAL METHODS

All of the calculations were performed using the NWChem computational chemistry package.[22] Structural optimizations were based on the DFT/B3LYP level of theory[23] and 6-31++G** basis set.[24] Molecular orbital analysis of resulting configurations was performed with the natural bond orbital (NBO)[25] module within NWChem and utilized the same DFT level of theory as structural optimizations. Similarly, NBO calculations were used to compute natural atomic charges used in charge analysis. Using DFT-optimized geometries, the final energies used in electron detachment calculations were calculated using the coupled cluster with perturbative triples (CCSD(T))[26] level of theory and aug-cc-pvdz basis set.[27] The vertical electron detachment energy (VDE) was determined as the energy difference between doublet monoanion and singlet dianion species both at the same optimized dianion geometry. The adiabatic detachment energy (ADE) was computed as the energy difference between doublet monoanion and singlet dianion species at their respective optimized geometries. Zero-point energy (ZPE) corrections to ADE values were calculated on the same level of theory as structural optimizations.

EXPERIMENTAL RESULTS

The experimental NIPE spectra of both DC_2^{2-} and Asp^{2-} species are shown in Figure 1. Measurements were performed at three wavelengths, 193, 266, and 355 nm. The Asp^{2-} spectrum at each wavelength is, in general, very similar to the respective one of DC_2^{2-}, showing that the detached electrons are from $-CO_2^-$ groups in both cases. Both 266 and 193 nm spectra showed two bands, X with its EBE spanning from 0 to 1 eV and A with its EBE between 1 and 2 eV. The two-band spectral pattern is similar to that from a previous study on dicarboxylate dianions.[14−18] The first band X corresponds to the ground and first excited state of the detached carboxylate radical, $-CO_2^{\bullet}$ by removal of one electron from the highest occupied molecular orbital (HOMO) (mainly a σ^* in-plane antibonding orbital) and from the HOMO−1 orbital (σ in-plane bonding combination) in the $-CO_2^-$ group, respectively; the second spectral band A is ascribed to the second excited state of $-CO_2^{\bullet}$ by detaching one electron from the HOMO−2 orbital with an out-of-plane antibonding π^* character.[28−30] Because the first band in each spectrum contains both ground and excited states, we could not determine the VDE from the spectra. However, we can estimate ADE by drawing a straight line along the rising edge of each spectrum and adding instrumental resolution to the crossing point with the binding energy axis. The ADE was estimated to be 0.00 ± 0.05 eV for DC_2^{2-}, and a slightly positive ADE of 0.05 ± 0.05 eV was observed for Asp^{2-} (Table 1). Therefore, the substitution of amine in Asp^{2-} for one hydrogen atom in DC_2^{2-} results in a 50 meV increase in ADE. Although the ADE increase is small, Asp^{2-} is characterized by a strong dianion beam from electrospray. We never got a strong DC_2^{2-} anion beam under the same conditions. This confirms that DC_2^{2-} is only a "barely" stable dianion and Asp^{2-} is a stable dianion in the gas

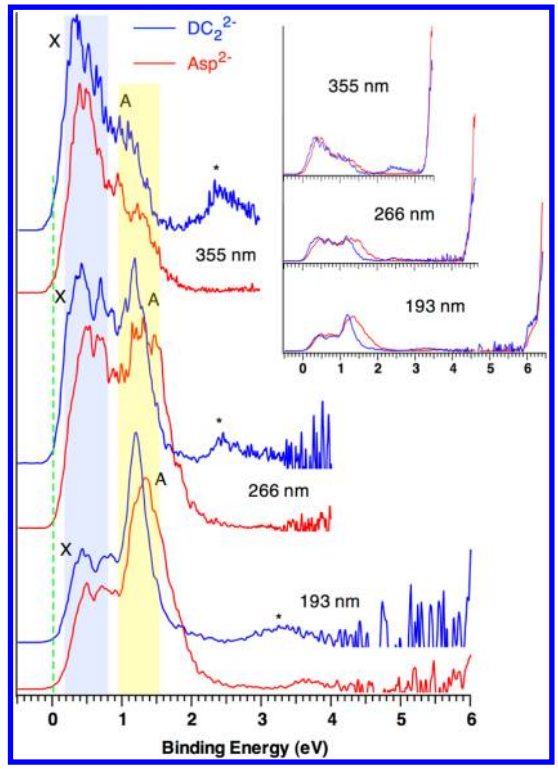

Figure 1. The 20 K photoelectron spectra of DC_2^{2-} (blue) and Asp^{2-} (red) at 355 (3.496 eV), 266 (4.661 eV), and 193 nm (6.424 eV). A dashed green line is drawn along the threshold region in the spectra to help identify the subtle shift in binding energy between DC_2^{2-} and Asp^{2-}. The weak bands denoted with ∗ at the higher EBE region are features from detachment of the product monoanion (or the fragment anion) by a second photon (see the text). (Inset) The same set of spectra of DC_2^{2-}/Asp^{2-} at three different wavelengths but plotted out to the respective photon energy limits, showing enhancement for the near 0 eV electrons due to dissociative secondary autodetachment for Asp^{2-} (see the text for details). The intensities of fast electrons due to direct detachment are scaled to match those of DC_2^{2-}.

dx.doi.org/10.1021/jp505439b | J. Phys. Chem. A 2014, 118, 5256−5262

Table 1. Experimental and Calculated ADEs, Calculated VDEs, Barriers E_a for Electron Autodetachment of DC_2^{2-}, Asp^{2-}, DC_3^{2-}, and Glu^{2-}, and Relaxation Energies E_r of Singly Charged Radical Anions

	ADE (eV)				
	expt.[a]	calc.[b]	calc. VDE (eV)[c]	calc. E_a (kcal/mol)[d]	calc. E_r (kcal/mol)[e]
DC_2^{2-}	0.00 (5)	−0.08 (−0.11)	0.31	1.4	8.9
Asp^{2-}	0.05 (5)	−0.05 (−0.10)	0.62	3.3	15.5
DC_3^{2-}	0.50 (5)	0.48 (0.46)	0.83	11.3	8.1
Glu^{2-}	0.65 (5)	0.62 (0.56)	1.04	14.8	9.7

[a]Obtained by drawing a straight line along the rising edge of each spectrum and adding instrumental resolution to the crossing point with the binding energy axis. The numbers in parentheses represent experimental uncertainty in the last digit. [b]Calculated as the energy difference of the doublet monoanion and singlet dianion states at their respective optimized geometry at the CCSD(T)/aug-cc-pvdz//B3LYP/6-31++G** level of theory. ZPE-corrected values are shown in parentheses. [c]Computed as the energy difference of the doublet monoanion and singlet dianion states both at the optimized dianion's geometry at the CCSD(T)/aug-cc-pvdz//B3LYP/6-31++G** level of theory. [d]Energy barrier for the electron-transfer process from the optimized singlet dianion to the optimized doublet monoanion estimated using Marcus theory (see the text). [e]Relaxation energy of the doublet monoanion from the initial dianion geometry to its own optimized geometry.

phase. All spectra show cutoffs in the higher EBE regime, and the second spectral bands at 355 nm are severely suppressed in intensity compared to that at 266 and 193 nm. These are due to the universal existence of a repulsive Coulomb barrier (RCB) in MCA,[31−35] preventing slow electrons from being directly detached. The relatively weak, but visible bands (denoted with ∗) at the higher EBE region are features from detachment of the product monoanion (or the fragment anion) by a second photon,[16,36] but such bands are largely absent in the 355 and 266 nm Asp^{2-} spectra.

Figure 2 provides comparison of NIPE spectra between DC_3^{2-} and Glu^{2-}. Two broad bands, X at EBEs of 0.5−1.4 eV and A at EBEs of 1.5−2.1 eV, are observed at 193 nm for DC_3^{2-} and Glu^{2-} and show a very similar spectral pattern. The ADEs were estimated to be 0.50 ± 0.05 and 0.65 ± 0.05 eV for DC_3^{2-} and Glu^{2-}, respectively (Table 1). Amine functionalization has induced a 0.15 eV increase in ADE from DC_3^{2-} to Glu^{2-}, significantly larger than the 0.05 eV increase observed from DC_2^{2-} to Asp^{2-}. The appreciable EBE blue shift of Glu^{2-} is the reason that the second band A is greatly suppressed at 266 nm and almost disappears at 355 nm compared to the respective DC_3^{2-} spectrum.

For both Asp^{2-} and Glu^{2-}, at first glance, the increase of binding energies compared to those of DC_2^{2-} and DC_3^{2-} would be most likely from the formation of the intramolecular N−H···O hydrogen bond between the amine group and the carboxylate group(s) to stabilize the dianion and make the binding energy higher. As found from our theoretical calculations, which will be discussed in the subsequent sections, this EBE increase also directly relates to the geometry relaxation introduced by addition of $-NH_2$ on the photodetached singly charged radical surfaces.

THEORETICAL RESULTS AND DISCUSSIONS

DC_2^{2-} and $DC_2^{\bullet-}$. The lowest-energy optimized structures of singlet (DC_2^{2-}) and doublet ($DC_2^{\bullet-}$) states of succinate are shown in Figure 3. Both singlet and doublet states are characterized by a staggered configuration of the carboxylate groups, in nearly perpendicular orientation to each other. Such a configuration would provide the most reduction in the Coulomb repulsion energy between the negatively charged oxygen atoms on the two ends of the molecule. We also note the alignment of the carboxylate groups with the adjacent CH bonds on the alkyl chain; the preference for such a configuration is seen for other dicarboxylates species considered this work.

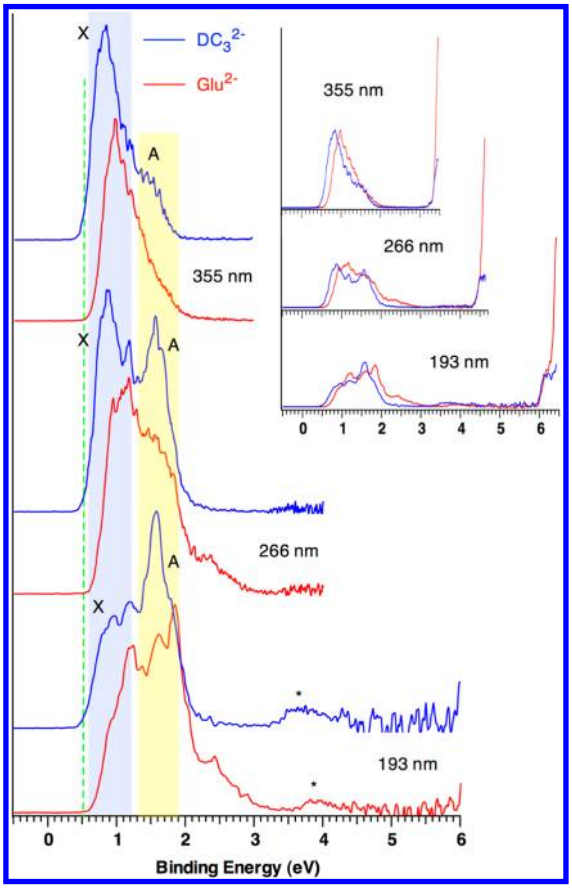

Figure 2. The 20 K photoelectron spectra of DC_3^{2-} (blue) and Glu^{2-} (red) at 355 (3.496 eV), 266 (4.661 eV), and 193 nm (6.424 eV). A dashed green line is drawn along the threshold region in the spectra to help identify the shift in binding energy between DC_3^{2-} and Glu^{2-}. The weak bands denoted with ∗ at the higher EBE region are features from detachment of the product monoanion (or the fragment anion) by a second photon (see the text). (Inset) The same set of spectra of DC_3^{2-}/Glu^{2-} at three different wavelengths but plotted out to the respective photon energy limits, showing enhancement for the near 0 eV electrons due to dissociative secondary autodetachment for Glu^{2-} (see the text for details). The intensities of fast electrons due to direct detachment are scaled to match those of DC_3^{2-}.

The calculated VDE for DC_2^{2-} of 0.31 eV compares well with that of the experimental spectrum. After the electron detachment event, the system is no longer at the equilibrium point on the potential energy surface, and the doublet radical

dx.doi.org/10.1021/jp505439b | J. Phys. Chem. A 2014, 118, 5256−5262

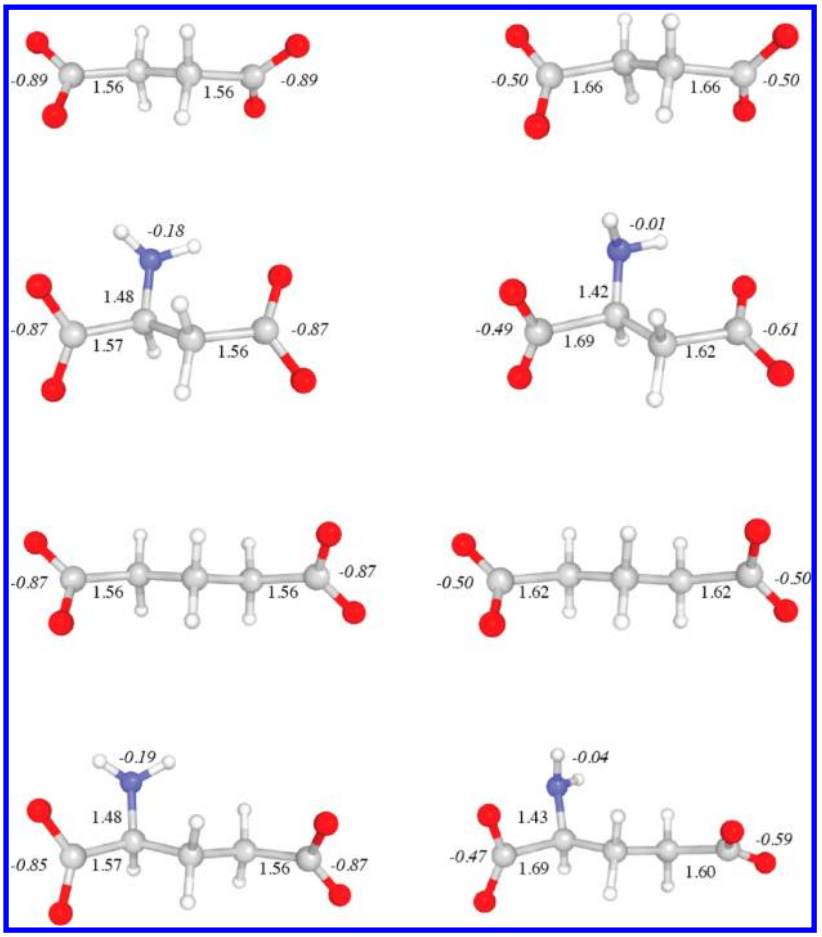

Figure 3. B3LYP/6-31++G** optimized structures of DC_2, Asp, DC_3, and Glu (top to bottom) of the singlet, doubly charged closed-shell (left) and doublet, singly charged open-shell states (right). Distances are in Angstrom units. NBO charges for $-CO_2$ and $-NH_2$ groups are indicated in italics.

anion evolves toward a more stable configuration. This relaxation results in relatively small structural differences and reflects the weakened interactions between the carboxylate and alkyl chain groups due to loss of an electron. The C−C bond between the two groups lengthens slightly (+0.1 Å), and the ∠OCO carboxylate angle opens up (+7.5°). The energy of the relaxed doublet state is slightly below the singlet state, which results in the small negative ADE in the range of −0.08 eV (−0.11 with ZPE correction), compared to the experimental estimate of 0.00 eV, which should be considered as an upper limit of true ADE.

Both experimentally estimated and computationally calculated ADEs suggest that the singlet dianion state DC_2^{2-} is unstable toward electron autodetachment. The existence of RCB in MCAs prevents spontaneous electron release, rendering these species finite tunneling lifetimes.[11,32] As noted earlier, experimental production of DC_2^{2-} was significantly more difficult than that of other dicarboxylate species considered in this work, raising the possibility of a thermally activated channel for electron autodetachment. While detailed analysis of this process is beyond the scope of this paper, a simple estimate of the barrier can be obtained from Marcus theory[37] (see Figure 4) using computed VDE and ADE values as

$$E_a = \frac{\mathrm{VDE}^2}{4(\mathrm{VDE} - \mathrm{ADE})} \quad (1)$$

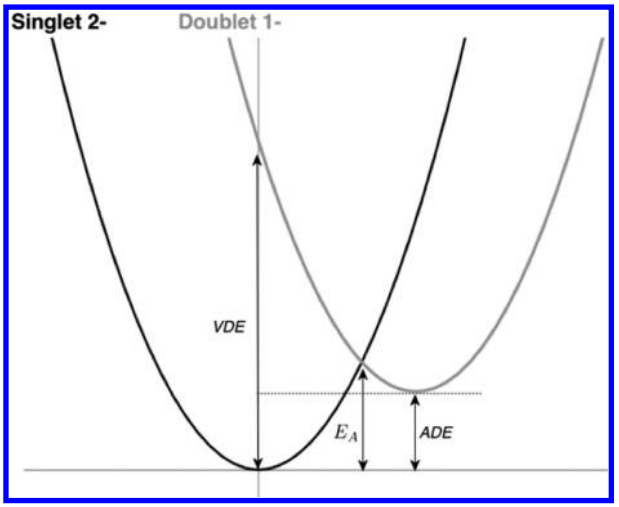

Figure 4. Schematic illustration of the Marcus-type relationship between the activation barrier and VDEs and ADEs.

For the autodetachment process of $DC_2^{2-} \rightarrow DC_2^{\bullet -}$, we obtain E_a = 1.4 kcal/mol (Table 1). This small barrier would be consistent with observed experimental instability as the DC_2^{2-} dianions were initially generated at ambient conditions and transported at room temperature before being stored into the cryogenic trap. During this time, a significant amount of the dianions could go over the barrier and be subject to electron autodetachment.

dx.doi.org/10.1021/jp505439b | J. Phys. Chem. A 2014, 118, 5256−5262

DC_3^{2-} and $DC_3^{\bullet-}$. Similar to succinate, the optimized structures of propionate singlet and doublet states are characterized by the staggered configuration of carboxylates aligned with the adjacent CH bonds. The calculated VDE value of 0.83 eV is consistent with that of the experimental spectra. The 0.52 eV increase of VDE, compared to DC_2^{2-}, is mainly related to the reduction of intramolecular Coulomb repulsion between two carboxylate end groups as a result of a longer alkyl chain, which results in a larger distance between the two charged centers in DC_3^{2-}.[14]

Relaxation of the doublet $DC_3^{\bullet-}$ state proceeds analogously to $DC_2^{\bullet-}$, consisting of the increased separation between carboxylate and alkyl groups and flattening of the ∠OCO carboxylate angle. As a result, the relaxation energy of $DC_3^{\bullet-}$ is similar to that of $DC_2^{\bullet-}$ (8.1 versus 8.9 kcal/mol, Table 1). The calculated ADE for DC_3^{2-} is 0.48 (0.46 with ZPE) eV, agreeing well with the experimental value of 0.50 eV. Overall, our results suggest that observed differences between DC_2^{2-} and DC_3^{2-} are largely electrostatic in nature, driven by differences in the intramolecular Coulomb repulsion mentioned above. The net effect is the shift of the spectrum by ∼0.5 eV. As a result of the increased stability of the dianion state, DC_3^{2-} is characterized by a high activation barrier toward electron detachment (E_a = 11.3 kcal/mol).

Asp^{2-} and $Asp^{\bullet-}$. The Asp^{2-} is obtained through the substitution of one of the α-methylene hydrogen atoms in DC_2^{2-} by the amine group ($-NH_2$). Given the relatively short length of the alkyl chain in this case, the amine group has an opportunity to establish hydrogen bonds with both carboxylates. The amine group occupies inequivalent position with respect to carboxylates, and the O···N distances for the closest and distant carboxylates are 2.74 and 2.94 Å, respectively. This distance disparity, however, is somewhat compensated for by the differences in hydrogen bond angles. The hydrogen bond to the closest carboxylate group is fairly strained (∠NHO = 112°), and more favorable alignment (∠NHO = 141°) can be established with a distant carboxylate group (O···N = 2.94 Å). Overall, the addition of an amine group has little effect on the structure of the dianion singlet state, and the structural parameters of Asp^{2-} are very similar to those of DC_2^{2-} (Figure 3). The presence of hydrogen bonds in Asp^{2-} should result in greater stabilization of the double charged singlet state. This is reflected in the calculated VDE value of 0.62 eV, which is 0.3 eV higher than that of DC_2^{2-} (Table 1). This is also in accord with the experimental findings, which exhibit the shift of the maximum position of the first band for Asp^{2-} to higher energy compared to that of DC_2^{2-} (Figure 1).

Charge analysis shows that the initial reduction in electron density upon one electron detachment is split nearly equally between both carboxylate groups. This is similar to what has been observed for the succinate case. However, upon relaxation of the doublet $Asp^{\bullet-}$ state, the balance is shifted toward the distant (with respect to NH_2) carboxylate group, making it more negatively charged (see Figure 3). This charge migration is accompanied by the rotation of NH_2 toward distant $-CO_2^-$, which significantly impacts the hydrogen bond angle to the closest carboxylate (∠NHO = 96°). The changes that accompany relaxation of the doublet state in $Asp^{\bullet-}$ can be understood by considering the electron-donating properties of the amine group. The loss of electron density in the vertical detachment process weakens the bond between the carboxylate and alkyl group. On the side adjacent to the amine group, this allows for an establishment of a resonance structure where a nitrogen lone pair can participate in the formation of a partial double bond with an adjacent carbon atom. This conclusion is supported by the NBO analysis of the relaxed doublet state that shows the appearance of an additional C−N bonding orbital. The evidence for the increased C−N bond order is also seen in the structure of the relaxed doublet state, where we observe the shortening of the C−N bond (−0.06 Å) (Figure 3). The resonance structure further weakens the interaction between alkyl and carboxylate groups on the side closest to NH_2, which is observed in its longer length, 1.69 versus 1.62 Å on the opposite side. The net result of these changes is significant stabilization of the energy of the doublet state (the relaxation energy is calculated as 15.5 kcal/mol, Table 1). This brings it slightly below that of the singlet Asp^{2-}, resulting in a small negative ADE value of −0.05 (−0.10 with ZPE) eV (Table 1). The calculated positive ADE change from DC_2^{2-} to Asp^{2-} of +0.03 (+0.01) eV is consistent with the experimental observation of +0.05 eV (Table 1).

For low ADE values (ADE ≪ VDE), the electron autodetachment barrier is driven primarily by the VDE value, $E_a \approx$ VDE/4. Thus, the elevated VDE values of Asp^{2-} compared to those of DC_2^{2-} have a significant effect on the electron autodetachment activation energy. The estimated reaction barrier of 3.3 kcal/mol (see eq 1) is much higher than 1.4 kcal/mol for DC_2^{2-} (Table 1). This could explain the fact that an abundant Asp^{2-} beam is observed in the gas phase, in contrast to the fact that only very weak DC_2^{2-} can be generated under similar experimental conditions.

Glu^{2-} and $Glu^{\bullet-}$. Obtained through amine group functionalization of DC_3^{2-}, Glu^{2-} has a longer alkyl chain length than Asp^{2-}. This places the amine group in a much more asymmetrical position with respect to carboxylates. Only the carboxylate closest to the amine group can participate in hydrogen bonding, parameters of which are slightly better (N···O = 2.7 Å, ∠NHO = 118°) than those found in Asp^{2-}. The distant carboxylate adopts a configuration where it aligns with the adjacent CH bond.

The calculated VDE value for the lowest-energy singlet Glu^{2-} state is 1.04 eV, which compares well with the experimental spectrum. The amine group addition leads to the increase of VDE by 0.21 eV (relative to DC_3^{2-}), consistent with the blue shift for the peak position of the X band for Glu^{2-}. However, this VDE increase for $DC_3^{2-} \rightarrow Glu^{2-}$ is 0.1 eV (2.3 kcal/mol) smaller than what we observed for $DC_2^{2-} \rightarrow Asp^{2-}$, which is consistent with the loss of one hydrogen bonding contact in Glu^{2-}. Relaxation of the doublet $Glu^{\bullet-}$ state proceeds analogous to $Asp^{\bullet-}$ and is accompanied by charge migration to the distant carboxylate group (see Figure 3). As with $Asp^{\bullet-}$, these changes facilitate the formation of the resonance structure. We observe similar reduction in C−N bond length (−0.05 Å) and elevated elongation of the C−C bond between the alkyl and carboxylate groups on the side closest to NH_2, 1.69 versus 1.60 Å on the opposite side. Unlike $Asp^{\bullet-}$, however, the resulting stabilization of the doublet state is less pronounced. The main reason for this difference is likely to be related to the increased energetic costs of charge migration further away from the amine group. The reorganization energy for $Glu^{\bullet-}$ is 9.7 kcal/mol compared to 15.5 kcal/mol for $Asp^{\bullet-}$ (Table 1). The calculated ADE value for Glu^{2-} is 0.62 (0.56 with ZPE) eV, which is ∼0.1 eV above that of DC_3^{2-}. A similar trend is exhibited in the experimental spectra, which indicates a 0.15 eV ADE difference between DC_3^{2-} and Glu^{2-} (Table 1).

dx.doi.org/10.1021/jp505439b | J. Phys. Chem. A 2014, 118, 5256−5262

Impact of Amine Functionalization on Decarboxylation of Radical Monoanions. It has been previously demonstrated[18] that one possible reaction channel in the post-photodetachment evolution of the monoanion radical dicarboxylate species may involve a autodecarboxylation reaction consisting of the loss of the CO_2 group, that is, $^{\bullet}O_2C-(CH_2)_n-CO_2^- \rightarrow O_2C + {}^{\bullet}(CH_2)_n-CO_2^-$. Similar decarboxylation of carboxyl radicals ($R-COO^{\bullet} \rightarrow R^{\bullet} + CO_2$) has been studied in details by Continetti and co-workers using photoelectron−photofragment coincidence spectroscopy.[38,39] The resulting monoanion radical $[^{\bullet}(CH_2)_n-CO_2^-]$ species are no longer subject to RCB effects and are expected to be highly unstable toward electron autodetachment. The spectroscopic signature of these secondary dissociative autodetachment events would be the appearance of near 0 eV kinetic energy slow electrons at the photon energy limits.[18] These zero kinetic energy electrons were indeed detected in the 266 nm NIPE spectra of DC_2^{2-} and DC_3^{2-} (see insets in Figures 1 and 2). In fact, they exist also in the 355 and 193 nm spectra, suggesting that the secondary dissociative autodetachment is thermodynamically favorable, independent of the photon energy used.

As suggested by the computational results discussed earlier in the paper, the addition of an amine group weakens significantly the binding of the adjacent carboxylate group in the monoanion doublet state. Structurally, this is manifested in the elongation the C−C bond between the alkyl and carboxylate on the side closest to NH_2 for both $Asp^{\bullet-}$ and $Glu^{\bullet-}$ radical anions. If this is indeed the case, one would expect that the autodecarboxylation reaction would be enhanced compared to their parent DC_2 and DC_3 dicarboxylate species. This is precisely the situation observed experimentally. Analysis of the spectra for Asp^{2-} shows the presence of near 0 eV secondary electron emission, the intensity of which is significantly stronger than that for DC_2^{2-} at all three wavelengths investigated here, 355, 266, and 193 nm (Figure 1 inset). Similar observation applies to Glu^{2-}; however, in this case, we see a much more dramatic increase in intensities of the zero kinetic energy secondary electron emission between DC_3^{2-} and Glu^{2-} (Figure 2 inset and Figures S1−S3, Supporting Information). These results provide further evidence that the addition of the amine group weakens the binding of the adjacent CO_2. More detailed investigation of these processes is currently under investigation.

CONCLUSIONS

Motivated by the ubiquity and important biological functions of aspartate and glutamate, we carried out a joint NIPES and computational study to examine the amine functionalization effects through comparison to their dicarboxylate counterparts, that is, succinate and propionate. Our results show that the introduction of an amine group has markedly different effects on the singlet and doublet potential energy surfaces of the two species. For singlet states, it results in the creation of $^-O\cdots H-N$ intramolecular H-bond(s) and leads to the increase of vertical electron binding energies relative to their respective dicarboxylates. For the doublet states, the main effect is the appearance of a resonance structure, which weakens the binding of the adjacent carboxylate group. The inherent asymmetry of amine group placement leads to different impact on shorter (Asp) and longer (Glu) chain species, which is exhibited in the observed variations of ADE. The reduced binding of the carboxylate group observed computationally suggests the increase in the rate of the post-photodetachment autodecarboxylation reaction of radical species, which is confirmed experimentally by the enhanced production of near 0 eV kinetic energy electrons. We believe that the obtained electron binding energies, molecular structures, as well as the potential impact on the decarboxylation pathway reported in this study will prove useful in increasing our understanding of the chemical roles played by aspartic and glutamic acids in the fundamental biological processes.

ASSOCIATED CONTENT

Supporting Information

Comparison of the 20 K photoelectron spectra of DC_2^{2-}/Asp^{2-} and DC_3^{2-}/Glu^{2-} at 355 (Figure S1), 266 (Figure S2), and 193 nm (Figure S3), showing enhancement for the near 0 eV electrons due to dissociative secondary autodetachment for Asp^{2-} and Glu^{2-}. This material is available free of charge via the Internet at http://pubs.acs.org.

AUTHOR INFORMATION

Corresponding Authors

*E-mail: marat.valiev@pnnl.gov (M.V.).
*E-mail: xuebin.wang@pnnl.gov (X-B-W.).

Present Address

#G.-L.H. and X.-Y.K.: Beijing National Laboratory for Molecular Sciences, State Key Laboratory of Molecular Reaction Dynamics, Institute of Chemistry, Chinese Academy of Sciences, Beijing 100190, China.

Notes

The authors declare no competing financial interest.

ACKNOWLEDGMENTS

This work was supported by the Division of Chemical Sciences, Geosciences, and Biosciences, Office of Basic Energy Sciences, U.S. Department of Energy (DOE) and performed using EMSL, a national scientific user facility sponsored by DOE's Office of Biological and Environmental Research and located at Pacific Northwest National Laboratory, which is operated by Battelle Memorial Institute for the DOE.

REFERENCES

(1) Valiev, M.; Kawai, R.; Adams, J. A.; Weare, J. H. The Role of the Putative Catalytic Base in the Phosphoryl Transfer Reaction in a Protein Kinase: Frist-Principles Calculations. *J. Am. Chem. Soc.* **2003**, *125*, 9926−9927.
(2) Rusak, B.; Bina, K. G. Neurotransmitters in the Mammalian Circadian System. *Annu. Rev. Neurosci.* **1990**, *13*, 387−401.
(3) Coyle, J. T.; Puttfarcken, P. Oxidative Stress, Glutamate, and Neurodegenerative Disorders. *Science* **1993**, *262*, 689−695.
(4) Jiang, Y. X.; Lee, A.; Chen, J. Y.; Ruta, V.; Cadene, M.; Chait, B. T.; MacKinnon, R. X-ray Structure of a Voltage-Dependent K^+ Channel. *Nature* **2003**, *423*, 33−41.
(5) Long, S. B.; Campbell, E. B.; MacKinnon, R. Crystal Structure of a Mammalian Voltage-Dependent Shaker Family K^+ Channel. *Science* **2005**, *309*, 897−903.
(6) Mass, W. P. M.; Nibbering, N. M. M. Formation of Doubly Charged Negative Ions in the Gas Phase by Collisionally-Induced "Ion Pair" Formation from Singly Charged Negative Ions. *Int. J. Mass Spectrom. Ion Processes* **1989**, *88*, 257−266.
(7) Kalcher, J.; Sax, A. F. Gas-Phase Stabilities of Small Anions — Theory and Experiment in Cooperation. *Chem. Rev.* **1994**, *94*, 2291−2318.
(8) Scheller, M. K.; Compton, R. N.; Cederbaum, L. S. Gas-Phase Multiply-Charged Anions. *Science* **1995**, *270*, 1160−1166.

(9) Boldyrev, A. I.; Gutowski, M.; Simons, J. Small Multiply Charged Anions as Building Blocks in Chemistry. *Acc. Chem. Res.* **1996**, *29*, 497−502.
(10) Dreuw, A.; Cederbaum, L. S. Multiply Charged Anions in the Gas Phase. *Chem. Rev.* **2002**, *102*, 181−200.
(11) Wang, X. B.; Wang, L. S. Experimental Search for the Smallest Stable Multiply Charged Anions in the Gas Phase. *Phys. Rev. Lett.* **1999**, *83*, 3402−3405.
(12) Wang, X. B.; Wang, L. S. Photoelectron Spectroscopy of Multiply Charged Anions. *Annu. Rev. Phys. Chem.* **2009**, *60*, 105−126.
(13) Wang, X. B.; Ding, C. F.; Wang, L. S. Photodetachment Spectroscopy of a Doubly Charged Anion: Direct Observation of the Repulsive Coulomb Barrier. *Phys. Rev. Lett.* **1998**, *81*, 3351−3354.
(14) Wang, L. S.; Ding, C. F.; Wang, X. B.; Nicholas, J. B. Probing the Potential Barriers and Intramolecular Electrostatic Interactions in Free Doubly Charged Anions. *Phys. Rev. Lett.* **1998**, *81*, 2667−2670.
(15) Skurski, P.; Simons, J.; Wang, X. B.; Wang, L. S. Experimental and Theoretical Investigations of the Stability of Two Small Gaseous Dicarboxylate Dianions: Acetylene Dicarboxylate and Succinate. *J. Am. Chem. Soc.* **2000**, *122*, 4499−4507.
(16) Minofar, B.; Mucha, M.; Jungwirth, P.; Yang, X.; Fu, Y. J.; Wang, X. B.; Wang, L. S. Bulk versus Interfacial Aqueous Solvation of Dicarboxylate Dianions. *J. Am. Chem. Soc.* **2004**, *126*, 11691−11698.
(17) Wang, X. B.; Yang, J.; Wang, L. S. Observation of Entropic Effect on Conformation Changes of Complex Systems under Well-Controlled Temperature Conditions. *J. Phys. Chem. A* **2008**, *112*, 172−175.
(18) Xing, X. P.; Wang, X. B.; Wang, L. S. Photoelectron Imaging of Doubly Charged Anions, $^{-}O_2C(CH_2)_nCO_2^{-}$ (n = 2−8): Observation of Near 0 eV Electrons Due to Secondary Dissociative Autodetachment. *J. Phys. Chem. A* **2010**, *114*, 4524−4530.
(19) Dessent, C. E. H.; Rigby, C. Exploring the Microscopic Solvation of Doubly Charged Anions: Symmetric or Asymmetric Solvation in the CO_2-$(CH_2)_4$-CO_2^{2-}·$(H_2O)_2$ Dicarboxylate Dianion Cluster? *Chem. Phys. Lett.* **2003**, *370*, 52−61.
(20) Herbert, J. M.; Ortiz, J. V. Ab Initio Investigation of Electron Detachment in Dicarboxylate Dianions. *J. Phys. Chem. A* **2000**, *104*, 11786−11795.
(21) Wang, X. B.; Wang, L. S. Development of a Low-Temperature Photoelectron Spectroscopy Instrument Using an Electrospray Ion Source and a Cryogenically Controlled Ion Trap. *Rev. Sci. Instrum.* **2008**, *79*, 073108/1−073108/8.
(22) Valiev, M.; Bylaska, E. J.; Govind, N.; Kowalski, K.; Straatsma, T. P.; Van Dam, H. J. J.; Wang, D.; Nieplocha, J.; Apra, E.; Windus, T. L.; de Jong, W. NWChem: A Comprehensive and Scalable Open-Source Solution for Large Scale Molecular Simulations. *Comput. Phys. Commun.* **2010**, *181*, 1477−1489.
(23) Becke, A. D. A New Mixing of Hartree−Fock and Local Density-Functional Theories. *J. Chem. Phys.* **1993**, *98*, 1372−1377.
(24) Dill, J. D.; Pople, J. A. Self-Consistent Molecular-Orbital Methods. 15. Extended Gaussian-Type Basis Sets for Lithium, Beryllium, and Boron. *J. Chem. Phys.* **1975**, *62*, 2921−2923.
(25) Glendening, E. D.; Badenhoop, J. K.; Reed, A. E.; Carpenter, J. E.; Bohmann, J. A.; Morales, C. M.; Weinhold, F. *NBO 5.0*; Theoretical Chemistry Institute, University of Wisconsin: Madison, WI, 2001.
(26) Bartlett, R. J.; Musial, M. Coupled-Cluster Theory in Quantum Chemistry. *Rev. Mod. Phys.* **2007**, *79*, 291−352.
(27) Kendall, R. A.; Dunning, T. H., Jr.; Harrison, R. J. Electron Affinities of the First-Row Atoms Revisited. Systematic Basis Sets and Wave Functions. *J. Chem. Phys.* **1992**, *96*, 6796−6806.
(28) Wang, X. B.; Woo, H. K.; Wang, L. S.; Minofar, B.; Jungwirth, P. Determination of the Electron Affinity of the Acetyloxyl Radical (CH_3COO) by Low-Temperature Anion Photoelectron Spectroscopy and Ab Initio Calculations. *J. Phys. Chem. A* **2006**, *110*, 5047−5050.
(29) Rauk, A.; Yu, D.; Armstrong, D. A. Carboxyl Free Radicals: Formyloxyl ($HCOO^{\bullet}$) and Acetyloxyl ($CH_3COO^{\bullet}$) Revisited. *J. Am. Chem. Soc.* **1994**, *116*, 8222−8228.
(30) Kim, E. H.; Bradforth, S. E.; Arnold, D. W.; Metz, R. B.; Neumark, D. M. Study of HCO_2 and DCO_2 by Negative Ion Photoelectron Spectroscopy. *J. Chem. Phys.* **1995**, *103*, 7801−7814.
(31) Wang, L. S.; Wang, X. B. Probing Free Multiply Charged Anions Using Photodetachment Photoelectron Spectroscopy. *J. Phys. Chem. A* **2000**, *104*, 1978−1990.
(32) Wang, X. B.; Wang, L. S. Observation of Negative Electron-Binding Energy in a Molecule. *Nature* **1999**, *400*, 245−248.
(33) Horke, D. A.; Chatterley, A. S.; Verlet, J. R. R. Effect of Internal Energy on the Repulsive Coulomb Barrier of Polyanions. *Phys. Rev. Lett.* **2012**, *108*, 083003/1−083003/5.
(34) Ehrler, O. T.; Weber, J. M.; Furche, F.; Kappes, M. M. Photoelectron Spectroscopy of C_{84} Dianions. *Phys. Rev, Lett.* **2003**, *91*, 113006/1−113006/4.
(35) Dreuw, A.; Cederbaum, L. S. Nature of the Repulsive Coulomb Barrier in Multiply Charged Negative Ions. *Phys. Rev. A* **2000**, *63*, 012501−1−13.
(36) Wang, X. B.; Nicholas, J. B.; Wang, L. S. Intramolecular Coulomb Repulsion and Anisotropies of the Repulsive Coulomb Barrier in Multiply Charged Anions. *J. Chem. Phys.* **2000**, *113*, 653−661.
(37) Marcus, R. A. Electron Transfer Reactions in Chemistry. Theory and Experiment. *Rev. Mod. Phys.* **1993**, *65*, 599−610.
(38) Clemente, T. G.; Continetti, R. E. Predissociation Dynamics of Formyloxyl Radical Studied by the Dissociative Photodetachment of HCO_2^{-}/DCO_2^{-} + hυ →H/D + CO_2 + e^{-}. *J. Chem. Phys.* **2001**, *115*, 5345−5348.
(39) Lu, Z.; Continetti, R. E. Dynamics of the Acetyloxyl Radical Studied by Dissociative Photodetachment of the Acetate Anion. *J. Phys. Chem. A* **2004**, *108*, 9962−9969.